

KINETICS AND MOLECULAR MODELING OF BIOLOGICALLY ACTIVE GLUTATHIONE COMPLEXES WITH LEAD(II) IONS

B. K. Singh, R. K. Sharma and B. S. Garg*

Department of Chemistry, University of Delhi, Delhi 110007, India

Lead(II) complexes of reduced glutathione (GSH) of general composition $[\text{Pb}(L)(X)] \cdot \text{H}_2\text{O}$ (where $L=\text{GSH}$; $X=\text{Cl}, \text{NO}_3, \text{CH}_3\text{COO}, \text{NCS}$) have been synthesized and characterized by elemental analyses, infrared spectra and electronic spectra. Thermogravimetric (TG) and differential thermal analytical (DTA) studies have been carried out for these complexes. Infrared spectra indicate deprotonation and coordination of cysteinyl sulphur with metal ion. It indicates the presence of water molecule in the complexes that has been supported by TG/DTA. The thermal behaviour of complexes shows that water molecule is removed in first step-followed removal of anions and then decomposition of the ligand molecule in the subsequent steps. Thermal decomposition of all the complexes proceeds via first order kinetics. The thermodynamic activation parameters, such as E^* , A , ΔH^* , ΔS^* and ΔG^* have been calculated. The geometry of the metal complexes has been studied with the help of molecular modeling for energy minimization calculation.

Keywords: differential thermal analysis, glutathione, lead(II) complexes, thermodynamic activation parameters, thermogravimetry

Introduction

Recent studies on determination of kinetic parameters from thermal data prompted us to analyze the variation in thermal stability of some metal complexes in terms of their structural parameters [1, 2]. This follows from our interest to investigate the thermal behaviour of metal glutathione complexes.

Metal complexes of glutathione (GSH) serve important functions in our biological systems and play a dominant role in protein metabolism. These are important constituents of enzymes, proteins and present in many parts of the biological system [3]. Glutathione (γ -glutamate-cystein-glycine, GSH) is the most important cellular thiol, which exists in mammalian cells and creates in the cell an important redox system [4–6]. It is reported to have anticancer activity [7–10] and glutathione enzyme (GE) was chosen as target molecules in antineoplastic chemotherapy treatment [11].

The binding of lead(II) by glutathione is the subject of interest for toxicity of metal ions in biological system [12–14]. Lead is a highly neurotoxic agent that causes functional and structural abnormalities in the brain [12]. Glutathione is a main molecule involved in the protection mechanism against itself and against reactive oxygen species generated by the metal. The study was carried out to investigate the effect of lead that stimulates glutathione system in several regions of adult rat brain [12]. The accumulation of thiol group (SH) in tissue also decreased lead toxicity [13]. Lead was administered to rats and total

glutathione and SH contents and metabolic turnover in their livers and kidneys were determined. The increased total content of glutathione and SH in the lead administered rat tissues increased the biological availability in rats of binding sites for the complexing of ionic lead. Therefore, glutathione and SH block the lead toxicity in rat tissues. The increased total glutathione content in bile was expected to protect the liver against lead toxicity [13].

Because of the presence of potential binding sites in glutathione (reduced), its coordination chemistry is complicated and the most definitive information has been obtained by using results from a combination of various techniques. Taking into account the complexity of the process, the kinetic calculations of all thermal decomposition reaction becomes important for the interpretation of structure of complicated molecules. We report herein the synthesis, spectral characterization, molecular modeling studies and thermal studies of biologically active glutathione with lead(II) ions.

Experimental

Preparation of complexes

Aqueous solution of lead(II) salts (0.001 M) was added with stirring to an aqueous solution of reduced glutathione (0.001 M). There is immediate formation of the white solid in good yield, which were filtered, washed with water and ethanol and dried over P_4O_{10} in vacuo.

* Author for correspondence: bibheshksingh@yahoo.co.in

Methods

The complexes were analyzed for C, H, N, S. Metal contents were estimated on an AA-640-13 Shimadzu flame atomic absorption spectrophotometer in solutions prepared by decomposing the complex in hot concentrated HCl. IR spectra were recorded on a Perkin-Elmer FTIR spectrophotometer spectrum 2000 in KBr and polyethylene pellets. The electronic spectra (900–200) nm of the complexes in solid state was recorded on Jasco-Unidec-430B double beam spectrophotometer. The molecular modeling calculation of metal complex was carried out with Hyperchem release 7.51 professional version. Rigaku Model 8150 Thermoanalyser (Thermafex) was used for simultaneous recording of TG-DTA curves at a heating rate of 5 K min⁻¹. For TG, the instrument was calibrated using calcium oxalate while for DTA, calibration was done using indium metal, both of which were supplied along with the instrument in ambient condition. A flat bed type Al-crucible was used with α -alumina (99% pure) as the reference material for DTA. The number of decomposition steps was identified using TG. The activation energy and Arrhenius constant of the degradation process was obtained by Coats and Redfern method [15]. Apparent activation entropy was calculated by Zsakó method [16]. Lead(II) salts and glutathione were procured from Aldrich and were used as received. Solvents used were of analytical grade and were purified by standard methods.

Results and discussion

The general reaction for the preparation of the metal complexes is shown below:



where $M = \text{Pb(II)}$; $X = \text{Cl, NO}_3, \text{CH}_3\text{CO}_2, \text{SCN}$ and $L = \text{GSH}$.

All the complexes were found to be white crystalline substances, non-hygroscopic and insoluble in common organic solvents. Satisfactory results of ele-

mental analysis (Table 1) and spectral studies revealed that the complexes were of good purity. Various attempts to obtain the single crystals have so far been unsuccessful.

Potentiometric studies

In order to visualize the nature of the complexation equilibria and to evaluate the thermodynamic parameters of complexes of lead(II) ions with glutathione has been studied [17]. Species distribution curves of complexes have been plotted as a function of pH, which showed that there is no significant complexation up to pH 3.38. At pH 3.39 formation of ML complex started. Percentage of ML was maximum (~78%) around pH 3.46. After which the percentage of ML started decreasing and fell to zero at pH~12.0. The studies confirms the exact pH values at which complexation occurs.

Infrared spectra

The IR spectra of the ligand and metal complexes are shown in Figs 1a–e. The results indicate that the glutathione (GSH) shows a strong band at 2525 due to ν_{SH} , which is absent in the spectra of the complexes indicating the deprotonation and coordination of the thiol group [18]. This has been confirmed by the appearance of $\nu_{\text{Pb-S}}$ band at 390–370 cm⁻¹ in all the complexes suggesting the binding of metal through sulphur [19]. In glutathione, the band at 1713 cm⁻¹ is assigned to the $>\text{C}=\text{O}$ stretching vibration of the $-\text{COOH}$ group of the glycine residue, is shifted to lower frequency, indicating the coordination of $-\text{COOH}$ group of glycine with metal ions in all the complexes [19]. The doublet peaks, appearing at 3347(s) and 3252(s) cm⁻¹ due to symmetric stretching vibrations of the peptide group [20] merged into a single band in all complexes in the region 3275–3265 cm⁻¹. The N–H stretching frequency at 3026 cm⁻¹ in the free ligand in a hydrogen bonded NH_3^+ in zwitter ion $-\text{OOC}-\text{C}-\text{NH}_3^+$ of the amino acid moiety [21] does not show any considerable shift in complexes, indicating the non participation of this N–H group. All complexes showed broad

Table 1 Analytical and electronic spectral data for Pb(II) – glutathione complexes

Complex	Yield/%	Colour	Analysis: found (calcd.)/%					Electronic spectral assign./nm
			C	H	N	S	Pb	
[Pb(L)(Cl)]·H ₂ O (C ₁₀ H ₁₇ N ₃ O ₇ SClPb)	78	white	21.19 (21.21)	2.95 (3.00)	7.38 (7.43)	5.59 (5.65)	36.55 (36.63)	380, 330, 225
[Pb(L)(NO ₃)]·H ₂ O (C ₁₀ H ₁₇ N ₄ O ₁₀ SPb)	76	white	20.20 (20.27)	2.80 (2.87)	9.39 (9.45)	5.37 (5.41)	34.96 (35.00)	382, 331, 228
[Pb(L)(CH ₃ CO ₂)]·H ₂ O (C ₁₂ H ₂₀ N ₃ O ₉ SPb)	75	offwhite	24.38 (24.45)	3.33 (3.40)	7.10 (7.13)	5.38 (5.43)	35.10 (35.18)	381, 332, 226
[Pb(L)(SCN)]·H ₂ O (C ₁₁ H ₁₇ N ₄ O ₇ S ₂ Pb)	74	white	22.40 (22.45)	2.84 (2.89)	9.47 (9.52)	10.79 (10.88)	35.15 (35.21)	380, 333, 226

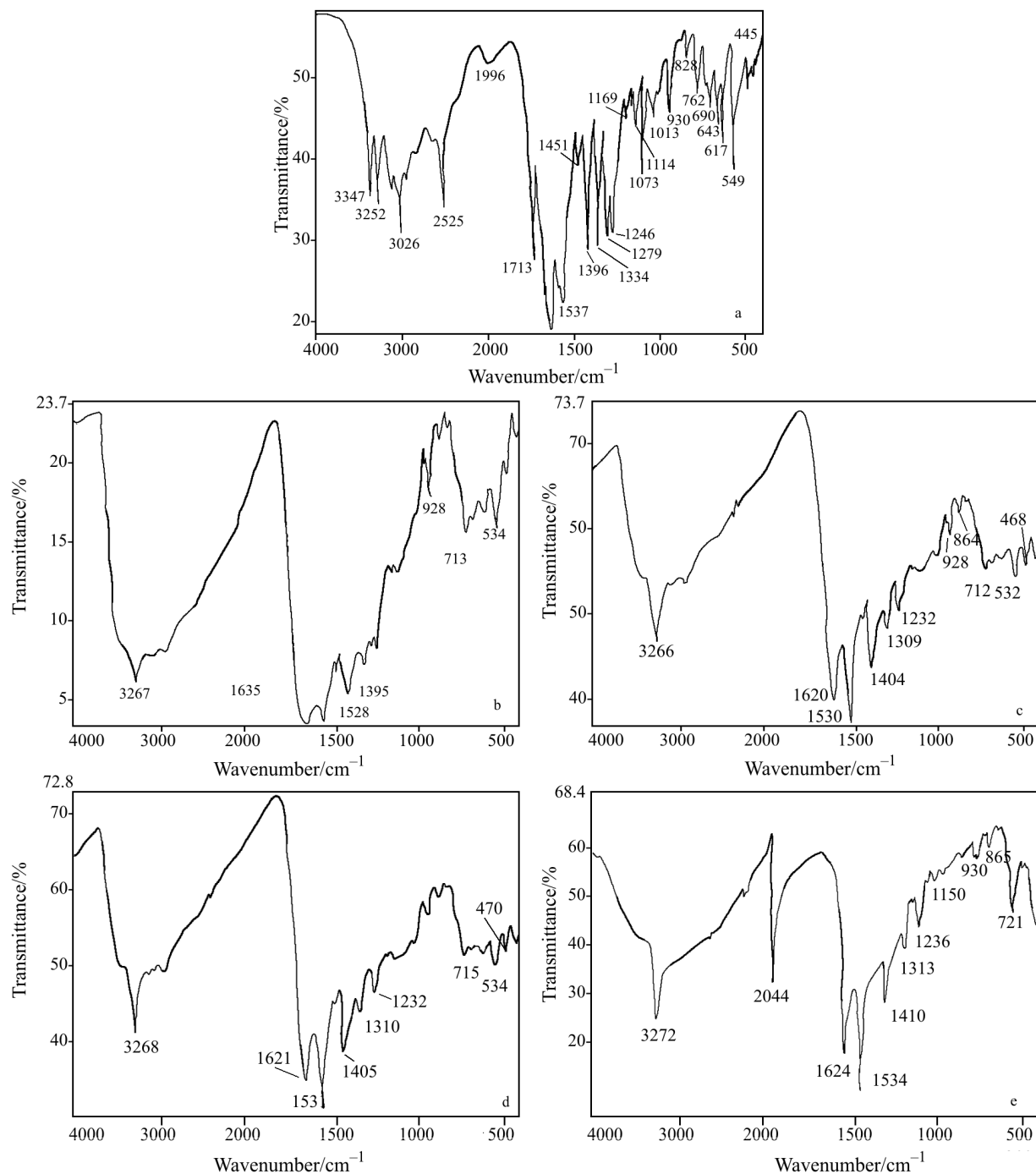


Fig. 1 IR spectrum of a – GSH, b – $[\text{Pb}(\text{L})(\text{Cl})]\cdot\text{H}_2\text{O}$, c – $[\text{Pb}(\text{L})(\text{NO}_3)]\cdot\text{H}_2\text{O}$, d – $[\text{Pb}(\text{L})(\text{CH}_3\text{CO}_2)]\cdot\text{H}_2\text{O}$ and e – $[\text{Pb}(\text{L})(\text{SCN})]\cdot\text{H}_2\text{O}$

band around 3400 cm^{-1} due to ν_{OH} from water molecules. This band is absent in the ligand. The band at 1665 cm^{-1} in the GSH is assigned to the $>\text{C}=\text{O}$ stretching of the peptide bonds. This band has been shifted to lower frequency at 1640 cm^{-1} which indicates the coordination of the $>\text{C}=\text{O}$ group with lead ion [20].

The $\text{C}=\text{O}$ and $\text{C}-\text{O}$ stretching frequency at $1600(\text{s})$ and $1396(\text{s})\text{ cm}^{-1}$ in glutathione, are assigned to $\nu_{\text{as}(\text{CO}_2)}$ and $\nu_{\text{s}(\text{CO}_2)}$ modes of the carboxylate group

and these bands show considerable shift in all the complexes [22, 23].

The acetate complex has band at 1621 and 1405 cm^{-1} that can be assign to $\nu_{\text{as}(\text{CO}_2)}$ and $\nu_{\text{s}(\text{CO}_2)}$ fundamental stretching bands, respectively, which are in agreement with the acetate group being monodentate [22, 24]. Because the difference $\Delta[\Delta=\nu_{\text{as}(\text{CO}_2)}-\nu_{\text{s}(\text{CO}_2)}]$ is $1621-1405=216\text{ cm}^{-1}$. The band at 1405 cm^{-1} is due to the $\nu_{\text{s}(\text{CO}_2)}$ mode of both acetate and L^{2-} ligand.

In thiocyanate complex, the band at 2044, 865, 475 and 258 cm^{-1} can be assigned to $\nu_{\text{C}\equiv\text{N}}$, $\nu_{\text{C-S}}$, ν_{NCS} and $\nu_{\text{M-NCS}}$, respectively [25, 26].

Electronic spectra

The UV spectra showed that the band at 225 nm is associated to the $n \rightarrow \pi^*$ transition of carbonyl group [27]. The transition at around 330 nm has been assigned to a charge transfer due to carbonyl group to the metal [28]. The reflectance spectra at around 380 nm in all the complexes are due to the $\text{S}(\sigma) \rightarrow \text{M}(\text{II})$ charge transfer band [29]. In the spectra of the lead chloride ion the peak at 210 nm shifts to 225 nm after complexation that merge with the spectra of carbonyl group, good evidence for lead(II) chloro-glutathione complex [30] (Table 1).

Thermal decomposition kinetic analysis

The kinetic analysis parameters such as activation energy (E^*), enthalpy of activation (ΔH^*), entropy of activation (ΔS^*), free energy change of activation (ΔG^*) were evaluated graphically by employing the Coats–Redfern relation Eq. (1):

$$\log [-\log (1-\alpha) / T^2] = \log [AR / \theta E^*(1-2RT/E^*)] - E^*/2.3RT \quad (1)$$

where α is the mass loss up to the temperature T , R is the gas constant, E^* is the activation energy in

J mol^{-1} , θ is the heating rate and $(1-2RT/E^*) \cong 1$. A plot of left hand side of Eq. (1) vs. $1/T$ gives a slope from which E^* was calculated and A (Arrhenius constant) was determined from the intercept.

Thermoanalytical (TG, DTA) data of the complexes are given in Table 2. The correlations between the different decomposition steps of the complexes with the corresponding mass losses are discussed in terms of the proposed formula of the complexes.

The $[\text{Pb}(\text{L})(\text{Cl})] \cdot \text{H}_2\text{O}$ complex with the general formula $[\text{Pb}(\text{C}_{10}\text{H}_{15}\text{N}_3\text{O}_6\text{SCL}) \cdot \text{H}_2\text{O}$ is thermally decomposed in three successive decomposition steps (Fig. 2a). The first estimated mass loss of 3.0% within the temperature range (323–365 K) may be attributed to the loss of water molecule (calculated mass loss=3.1%). The energy of activation of this step is 83.15 J mol^{-1} . The DTA curve gives endothermic peak at 350 K (maximum peak temp.). The second step occurs within the temperature range 491–503 K with the estimated mass loss 16.5% (calculated mass loss=16.6%) are reasonably accounted for the decomposition of the $\text{HCl} + \text{NH}_3 + \text{CO}_2$. The energy of activation of this step is 84.10 J mol^{-1} . The DTA curve gives endothermic peak at 497 K. The third step of decomposition occurs within the temperature range 750–853 K with an estimated mass loss of 41.5% (calculated mass loss=42.3%) and activation energy is 84.94 J mol^{-1} , which corresponds to the loss of $\text{C}_9\text{H}_{11}\text{N}_2\text{O}_3\text{S}$ molecule leaving PbO residue. The DTA curve gives exothermic peak at 810 K (maximum

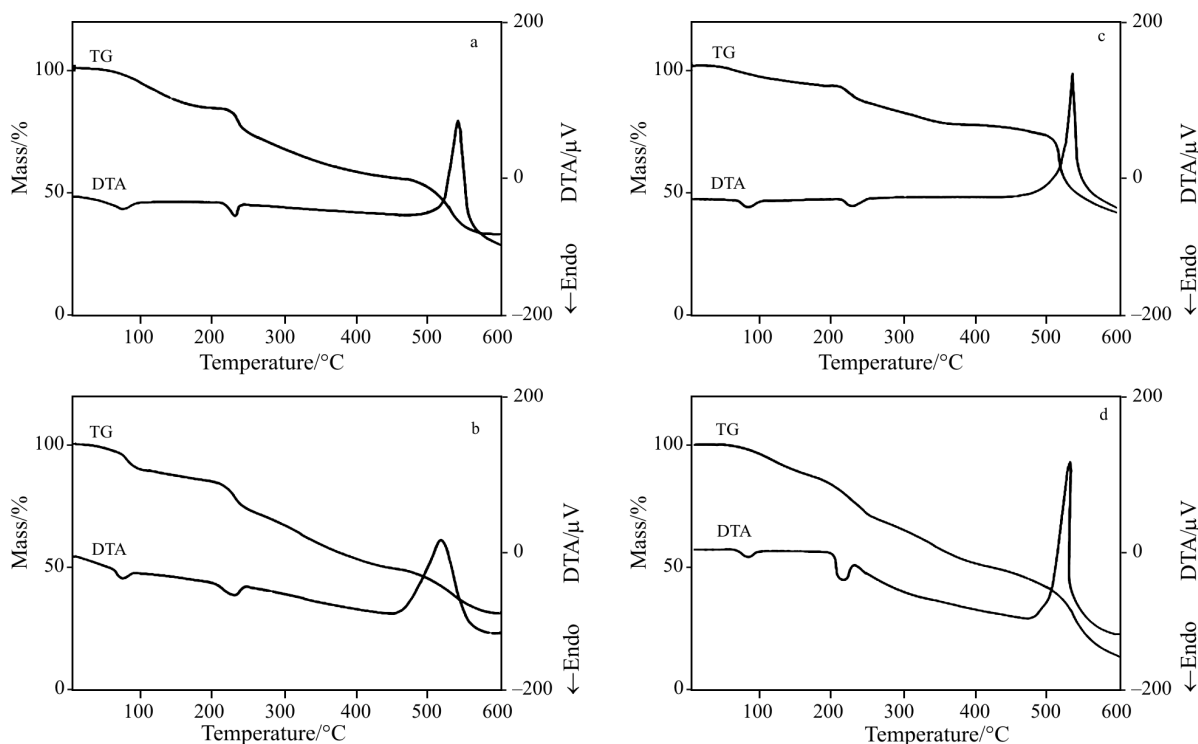


Fig. 2 TG/DTA curves of a – $[\text{Pb}(\text{L})(\text{Cl})] \cdot \text{H}_2\text{O}$, b – $[\text{Pb}(\text{L})(\text{NO}_3)] \cdot \text{H}_2\text{O}$, c – $[\text{Pb}(\text{L})(\text{CH}_3\text{CO}_2)] \cdot \text{H}_2\text{O}$ and d – $[\text{Pb}(\text{L})(\text{SCN})] \cdot \text{H}_2\text{O}$

Table 2 Thermoanalytical data (TG, DTA) of Pb(II)–glutathione complexes

Complex	Step	TG range/ K	DTA _{max} / K	Thermal effect	Mass loss obs. (calcd.)/%	Assignment	Metallic residue
[Pb(L)(Cl)]·H ₂ O	I	323–365	343	endo	3.0 (3.1)	H ₂ O	PbO
	II	491–503	497	endo	16.5 (16.6)	HCl+NH ₃ +CO ₂	
	III	750–853	810	exo	41.5 (42.3) 61.0 (62.0)	C ₉ H ₁₁ N ₂ O ₅ S	
[Pb(L)(NO ₃)]·H ₂ O	I	326–363	350	endo	12.5 (13.0)	H ₂ O+NO ₂ +1/2O ₂	PbO
	II	473–505	498	endo	9.8 (10.0)	NH ₃ +CO ₂	
	III	721–843	801	exo	42.0 (41.2) 64.3 (64.2)	C ₉ H ₁₂ N ₂ O ₄ S	
[Pb(L)(CH ₃ CO ₂)]·H ₂ O	I	345–371	355	endo	3.0 (3.1)	H ₂ O	PbO
	II	493–513	504	endo	13.8 (14.1)	CH ₄ +CO ₂ +NH ₃	
	III	752–850	812	exo	45.8 (45.0) 62.6 (62.2)	C ₁₀ H ₁₁ N ₂ O ₅ S	
[Pb(L)(SCN)]·H ₂ O	I	333–363	351	endo	3.1 (3.1)	H ₂ O	PbO
	II	400–520	492	endo	16.4 (16.6)	CH ₄ +SO ₂ +NH ₃	
	III	763–855	803	exo	42.7 (42.4) 62.2 (62.1)	C ₁₀ H ₈ N ₃ O ₃ S	

peak temp.). Total estimated mass loss 61.0% (total calculated mass=62.0%).

The [Pb(L)(NO₃)]·H₂O complex with the general formula [Pb(C₁₀H₁₅N₄O₉S)]·H₂O is thermally decomposed in three successive decomposition steps within the temperature range 323–873 K (Fig. 2b). The first decomposition step of estimated mass loss 12.5% within the temperature range 326–363 K may be attributed to the liberation of water molecule along with nitrate group as (NO₂+1/2O₂) gases (calculated mass loss is 13.5%). The energy of activation was 49.58 J mol⁻¹. The DTA curve gives endothermic peak at 350 K. The second step found within the estimated mass loss 9.8% (calculated mass loss 10.0%) which is responsibly accounted for the decomposition of NH₃+CO₂ molecule. The energy of activation was found to be 50.96 J mol⁻¹. The DTA curve gives endothermic peak at 498 K. The third step found in the TG range 721–843 K, which is responsibly accounted for the decomposition of rest of the ligand molecules (C₁₀H₁₂N₂O₅S) with a final residue PbO. The activation energy is found to be 45.87 J mol⁻¹. The DTA curve shows exothermic peak at 801 K (maximum peak temperature). The total estimated mass loss 63.8% (total calculated mass loss=63.4%).

The [Pb(L)(CH₃CO₂)]·H₂O complex with the general formula [Pb(C₁₂H₁₈N₃O₈S)]·H₂O was thermally decomposed again in three steps (Fig. 2c). The first estimated mass loss of 3.0% (calculated mass loss=3.1%) within the temperature range 345–371 K may be attributed to the liberation of water molecule. The energy of activation was found to be 53.72 J mol⁻¹. The DTA curve gives endothermic peak at 355 K. The second estimated mass loss 13.8% (calculated mass loss=14.1%) in the temperature range 493–513 K may be attributed to the loss of acetate (as CH₄ and CO₂ gases) and NH₃ molecule of the ligand. The energy of activation of this step is 54.61 J mol⁻¹. The DTA curve gives endothermic peak at 504 K. The third step of decomposition occurs within the temperature range

513–850 K with an estimated mass loss of 45.8% (calculated mass loss= 45.0%) and activation energy 63.71 J mol⁻¹, which corresponds to the loss of C₁₀H₁₁N₂O₅S molecule of the ligand leaving PbO residue with a total estimated mass loss 62.6% (total calculated mass loss=62.2%). DTA curve shows exothermic peak at 812 K (maximum peak temp.).

The [Pb(L)(SCN)]·H₂O complex with the formula [Pb(C₁₁H₁₅N₄O₆S₂)]·H₂O was thermally decomposed in three successive decomposition steps (Fig. 2d). The first estimated mass loss 3.1% (calculated mass loss 3.1%) within the temperature range 333–363 K can be attributed to the liberation of water molecule. The energy of activation of this step is 54.80 J mol⁻¹. The DTA curve gives endothermic peak at maximum peak temperature 351 K. The second step occurs within the temperature range 400–520 K with an estimated mass loss 16.4% (calculated mass loss=16.6%) with an energy of activation 55.56 J mol⁻¹ which is reasonably accounted for the loss of CH₄+SO₂+NH₃ molecule. The DTA curve gives endothermic peak at 492 K. The third step occurs within the temperature range 520–855 K with an estimated mass loss 42.7% (calculated mass loss=42.4%) with an energy of activation 62.8 J mol⁻¹, which is reasonably accounted for the loss of rest of the ligand molecule, leaving PbO as residue with total estimated mass loss 62.2% (total calculated mass loss=62.1%). The DTA curve gives exothermic peak at 803 K.

The relevant data needed for plotting linearization curve are recorded in Table 3 and linearization plots are shown in Figs 3a–d. The calculation of heat of reaction (ΔH^*) (Table 4) from the DTA curves were done by using:

$$\Delta H^* = \Delta H(\text{muv}) 60 \cdot 10^{-6} M \text{ J mol}^{-1} \quad (2)$$

where M is the molar mass of the complex and muv =micro unit volt. The temperature dependent calibration coefficient was obtained from Curell equation [31]. The entropy of activation (ΔS^*) and the free

Table 3 Kinetic parameters from TG for Pb(II) – glutathione complexes

T/K	[Pb(L)(Cl)]·H ₂ O			[Pb(L)(NO ₃)]·H ₂ O			[Pb(L)(CH ₃ CO ₂)]·H ₂ O			[Pb(L)(SCN)]·H ₂ O		
	x	y	z	x	y	z	x	y	z	x	y	z
353				0.05	2.84	6.75						
366							0.05	2.73	6.78			
370										0.05	2.70	6.76
372	0.10	2.69	6.48									
381				0.07	2.63	6.66						
417										0.08	2.40	6.67
439	0.20	2.28	6.43									
481										0.13	2.08	6.58
502				0.20	1.99	6.42						
504							0.15	1.98	6.56			
511	0.25	1.96	6.32									
552	0.30	1.81	6.29									
556										0.20	1.80	6.48
562							0.20	1.78	6.49			
565				0.30	1.77	6.32						
592	0.35	1.69	6.27									
605				0.35	1.65	6.29						
643	0.40	1.56	6.26									
645							0.25	1.55	6.42			
671										0.35	1.49	6.38
746				0.57	1.34	6.18						
800										0.52	1.25	6.30
830	0.60	1.12	6.20									
841							0.55	1.19	6.31			

Table 4 Thermodynamic activation parameters for Pb(II) – glutathione complexes

Complex	Order/n	Steps	E*/J mol ⁻¹	A/s ⁻¹	ΔS*/J K ⁻¹ mol ⁻¹	ΔH*/J mol ⁻¹	ΔG*/kJ mol ⁻¹
[Pb(L)(Cl)]·H ₂ O	1	I	83.15	10.70·10 ⁵	-130.43	4.52	44.74
		II	84.10	7.52·10 ⁵	-136.44	14.02	67.83
		III	84.94	4.75·10 ⁵	-144.20	985.96	116.35
[Pb(L)(NO ₃)]·H ₂ O	1	I	49.58	2.81·10 ⁵	-141.71	5.63	49.60
		II	50.96	2.08·10 ⁵	-147.14	20.05	73.45
		III	45.87	1.05·10 ⁵	-156.77	28.95	125.60
Pb(L)(CH ₃ CO ₂)]·H ₂ O	1	I	53.72	5.28·10 ⁵	-136.58	4.83	48.49
		II	54.61	3.83·10 ⁵	-142.20	20.90	71.66
		III	63.71	3.20·10 ⁵	-147.60	698.29	120.55
[Pb(L)(SCN)]·H ₂ O	1	I	54.80	5.19·10 ⁵	-136.63	4.73	47.96
		II	55.56	3.79·10 ⁵	-142.02	19.89	69.89
		III	62.89	2.97·10 ⁵	-148.13	1363.39	120.46

energy change of activation (ΔG^*) were calculated using the following equation.

$$\Delta S^* = 2.303R[\log(Ah/kT)] \text{ J K}^{-1} \text{ mol}^{-1} \quad (3)$$

$$\Delta G^* = \Delta H^* - T \Delta S^* \text{ J mol}^{-1} \quad (4)$$

where k and h are the Boltzman and Plank constants, respectively. The calculated values of E^* , A , ΔS^* , ΔH^*

and ΔG^* for the decomposition steps are given in Table 4. The ΔS^* values were found to be negative, which indicate a more ordered activated state that may be possible through the chemisorptions of oxygen and other decomposition product. The negative values of the entropies of activation are compensated by the values of the enthalpies of activation, leading to almost the same values for the free energies of activation.

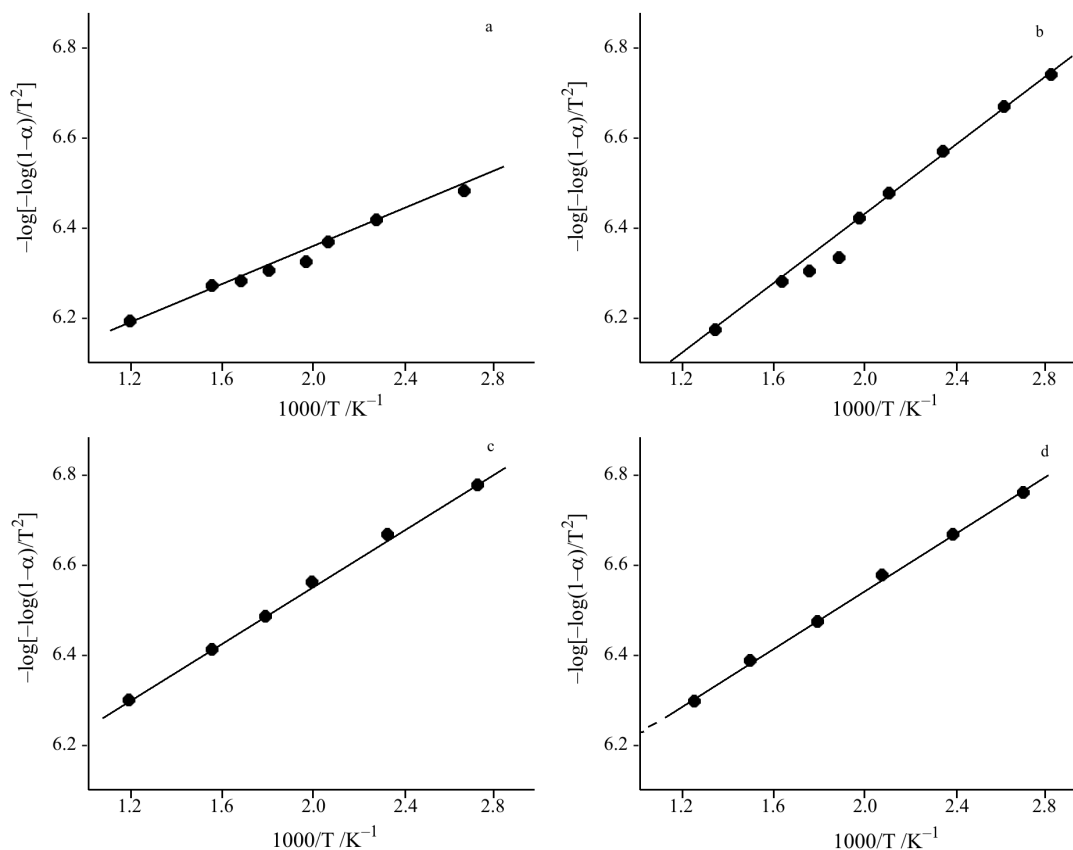


Fig. 3 a – Linearization plot of a – $[\text{Pb}(\text{L})(\text{Cl})]\cdot\text{H}_2\text{O}$, b – $[\text{Pb}(\text{L})(\text{NO}_3)]\cdot\text{H}_2\text{O}$, c – $[\text{Pb}(\text{L})(\text{CH}_3\text{CO}_2)]\cdot\text{H}_2\text{O}$ and d – $[\text{Pb}(\text{L})(\text{SCN})]\cdot\text{H}_2\text{O}$

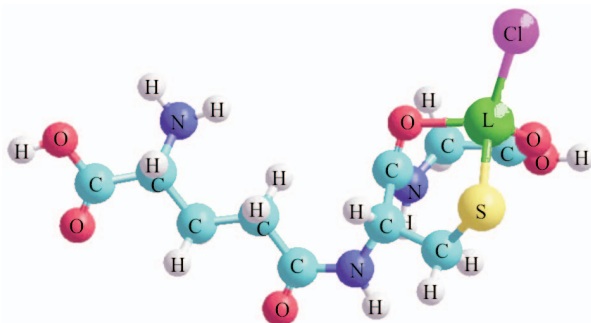


Fig. 4 Energy minimized structure of $[\text{Pb}(\text{L})(\text{Cl})]$ complex
S – sulphur, H – hydrogen, Cl – chlorine, C – carbon,
O – oxygen, N – nitrogen, L – lead

Molecular modeling studies

The molecular modeling calculations of $\text{Pb}(\text{II})$ –glutathione complexes were carried out [32] using an interactive program that allows for rapid structure building geometry optimization and molecular display. Energy minimization was repeated several times to find the global minimum. Molecular modeling studies, the energy minimization values for tetrahedral and without restricting the structure are almost equal i.e., 98.97 kcal. This supports tetrahedral geometry of metal complexes. Figure 4 shows the energy-minimized structure of $[\text{Pb}(\text{L})(\text{Cl})]\cdot\text{H}_2\text{O}$ complex.

Conclusions

Lead(II) complexes were found to be monomer and involved coordination through cysteine sulphur and carboxylate oxygen giving tetrahedral geometry. IR spectra indicate the presence of H_2O molecule in the complexes that has been supported by TG/DTA. Molecular modeling calculation for energy minimization optimizes geometry of the metal complexes shown in Fig. 4. TG data of the complexes were supplemented by DTA studies. Kinetic parameter shows the decomposition follows first order kinetics and proceeds in three-step decomposition.

Acknowledgements

One of the authors (B. K. Singh) is thankful to University Grants Commission, New Delhi, India for financial assistance under research award scheme.

References

- 1 D. N. Kumar and B. S. Garg, *J. Therm. Anal. Cal.*, 69 (2002) 607.
- 2 R. Sharma and N. K. Kaushik, *J. Therm. Anal. Cal.*, 78 (2004) 953.

- 3 P. C. Jocelyn, *Biochemistry of the SH group*, Academic Press, London 1972.
- 4 A. Verma, J. M. Simard, J. W. E. Worall and V. M. Rotello, *J. Am. Chem. Soc.*, 126 (2004) 13987.
- 5 K. D. Sugden and D. M. Stearns, *J. Environ. Path Toxicol. Oncol.*, 19 (2000) 215.
- 6 S. Grabner, J. Kosmrlj, N. Bukovec and M. Cemazer, *J. Inorg. Biochem.*, 95 (2003) 105.
- 7 K.P. Rice, P. G. Penketh, S. Krishnamurthy and A. C. Sartorelli, *Biochem. Pharmacology*, 69 (2005) 1463.
- 8 W. H. Ang, I. Khalaila, C. S. Allardyce, L. Juillerat-Jeanneret and P. J. Dyson, *J. Am. Chem. Soc.*, 127 (2005) 1382.
- 9 S. Kojima, K. Nakayama and H. Ishida, *J. Radiation Res.*, 45 (2004) 33.
- 10 B. Ning, C. Wang, F. Morel, S. Nowell, D. L. Ratnasinghe, W. Carter, F.F. Kadlubar and B. Coles, *Pharmacogenetics*, 14 (2004) 35.
- 11 Z. Kopanski, M. Grabowska, A. Kosiniak-Kamysz, J. Bertrand, L. Kolodziejski, W. Opoka and M. Schlegel-Zawadzka, *Biofactors*, 22 (2004) 79.
- 12 L. Struzynska, G. Sulkowski, A. Lenkiewicz and U. Rafalowska, *Folia Neuro-pathologica*, 40 (2002) 203.
- 13 K. Haraa, S. Ohmori, M. Nagano, Y. Kim and H. Miura, *Proc. ICMR Semin. (1994) (Proceed of Asia-Pacific Symp. on Environ. and Occupational Health)*, (1993) 99.
- 14 G. Li, Y. Jin, M. Zhao, X. Liu, A. Chem and Z. Xu, *Zhongguo Gongye Yixue Zazhi*, 16 (2003) 163.
- 15 A. W. Coats and J. P. Redfern, *Nature*, 201 (1964) 68.
- 16 J. Zsakó, *J. Phys. Chem.*, 72 (1968) 2406.
- 17 P. K. Singh, B. S. Garg, D. N. Kumar and B. K. Singh, *Ind. J. Chem.*, 40A (2001) 139.
- 18 J. Silver, M. Y. Hamed and I. E. G. Morrison, *Inorg. Chim. Acta*, 107 (1985) 169.
- 19 G. Domazetis, R. J Magee and B. D. James, *J. Organomet. Chem.*, 173 (1979) 357.
- 20 R. M. Silverstein, O. G. Bassler and T. C. Morrill, *Spectrophometric identification of organic compounds*, Wiley, New York 1974, p. 108.
- 21 H. Shindo and T. L. Brown, *J. Am. Chem. Soc.*, 87 (1965) 1904.
- 22 G. B. Deacon and R. J. Phillips, *Coord. Chem. Rev.*, 33 (1980) 227.
- 23 G. B. Deacon, F. Huber and R. J. Phillips, *Inorg. Chem. Acta*, 104 (1985) 41.
- 24 K. Nakamoto, *Infrared and Raman spectra of inorganic and coordination compounds*, 3rd Ed. Wiley, New York 1978.
- 25 V. B. Rana, D. P. Singh, P. Singh and M. P. Teotia, *Transition Met. Chem.*, 6 (1981) 36.
- 26 R. A. Bailey, S. L. Kozak, T. W. Michelsen and W. N. Mills, *Coord. Chem. Rev.*, 6 (1971) 407.
- 27 C. N. R. Rao, *Ultraviolet and visible spectroscopy*, Butterworth, London 1967, p. 190.
- 28 K. Nakamoto and S. J. McCarthy, *Spectroscopy and structure of metal chelate compounds*, John Wiley and Sons, USA 1968.
- 29 S. Akerfeldt and G. Lovgren, *Anal. Biochem.*, 8 (1964) 223.
- 30 H. Bendiab, J. Meullemeetre, M. J. Schwing and F. Vierling, *J. Chem. Res.*, (S) (1982) 280.
- 31 B. R. Curell, *Thermal Analysis*, Eds, R. F. Schenker and P. D. Garn, Vol. 2, Academic Press, New York 1969, p. 1185.
- 32 Hyperchem, Release 7.51 Professional version for window, Molecular Modeling system, Hyperchem. Inc., Canada 2005.

Received: July 8, 2005

Accepted: January 10, 2006

OnlineFirst: March 20, 2006

DOI: 10.1007/s10973-005-7156-z